

Regulation of Selective Autophagy Onset by a Ypt/Rab GTPase Module

Zhanna Lipatova¹, Natalia Belogortseva², Xiu Qi Zhang¹, Jane Kim², David Taussig²,
and Nava Segev^{1#}

Departments of Biochemistry and Molecular Genetics and Biological Sciences²,
University of Illinois at Chicago, 900 S. Ashland Ave, Chicago, IL 60607

Running title: Ypt1 and Atg11 in autophagy

Corresponding Author:

Nava Segev

Department of Biochemistry and Molecular genetics
University of Illinois at Chicago
Molecular Biology Research Building
900 South Ashland Avenue/ Chicago, Illinois 60607
Phone: 312-355-0142; Fax 312-413-0353; Email: nava@uic.edu

Abstract

The key regulators of intracellular trafficking, Ypt/Rab GTPases, are stimulated by specific upstream activators and, when activated, recruit specific downstream effectors to mediate membrane transport events. The yeast Ypt1 and its human functional homolog hRab1 regulate both endoplasmic reticulum (ER)-to-Golgi transport and autophagy. However, it is not clear whether the mechanism by which these GTPases regulate autophagy depends on their well-documented function in ER-to-Golgi transport. Here, we identify Atg11, the pre-autophagosomal structure (PAS) organizer, as a downstream effector of Ypt1 and show that the Ypt1-Atg11 interaction is required for PAS assembly under normal growth conditions. Moreover, we show that Ypt1 and Atg11 co-localize with Trs85, a Ypt1 activator subunit, and together they regulate selective autophagy. Finally, we show that Ypt1 and Trs85 interact on Atg9-containing membranes, which serve as a source for the membrane component of PAS. Together our results define the first Ypt/Rab module – comprising of activator, GTPase and effector – that orchestrates the onset of selective autophagy, a process vital for cell homeostasis. Furthermore, because Atg11 does not play a role in ER-to-Golgi transport, this is the first demonstration that Ypt/Rabs can regulate two independent membrane transport processes by recruiting process-specific effectors.

\body

Introduction

The conserved Ypt/Rab GTPases act as membrane organizers to regulate intracellular trafficking pathways. When stimulated by exchange factors termed GEFs, they interact with multiple downstream effectors, which mediate the different steps of vesicular trafficking [1, 2]. In yeast, Ypt1 is required for ER-to-Golgi transport [3-5] and the TRAPP I complex acts as its GEF [6, 7]. Rab1, the human functional homolog of Ypt1, also plays a role in ER-to-Golgi transport [8, 9]. Conserved tethering factors, like Uso1/p115, were identified as downstream effectors of Ypt1 and hRab1 in ER-to-Golgi transport [10, 11].

Autophagy is a cellular recycling process. In this process, a double membrane surrounds parts of the cytoplasm including cellular organelles to form the autophagosome, which fuses with the lysosome (vacuole in yeast), where macromolecules are degraded. Under stress conditions, like starvation, non-selective autophagy is induced [12]. In contrast, selective autophagy, in which specific cellular components are recycled, plays a role in cell homeostasis and is, therefore, important for human development and disease [13]. The best-characterized type of selective autophagy is the cytosol-to-vacuole (CVT) pathway, which delivers specific enzymes from the cytoplasm to the vacuole under normal growth conditions. A conserved set of autophagy-specific proteins, Atgs, is required for the different types of autophagy. All types of autophagy start with the formation of the pre-autophagosomal structure, PAS, which was originally defined as a conserved multi-protein complex. More recently it was suggested that Atg9, an integral-membrane protein required for all types of autophagy, supplies the membrane component to PAS [14]. At present, it is not clear how the

autophagy-specific and the membrane-trafficking machinery intersect to generate the autophagosome.

While several Ypt/Rabs were implicated in autophagy, the molecular mechanisms that underlie their function in this process are mostly unknown. Ypt1 and its mammalian homolog Rab1 play a role in autophagy [15, 16], and Trs85, in the context of the TRAPP III complex, can act as a Ypt1 GEF in this process [17]. However, the molecular mechanism by which Ypt1 and Rab1 regulate autophagy is unknown, and it is not clear whether it is dependent on their well-documented function in ER-to-Golgi transport.

Atg11 is a PAS scaffold protein required for different types of selective autophagy including CVT [18, 19]. Here, we use a combination of biochemistry, genetics and imaging approaches to identify Atg11 as a downstream effector of Ypt1 and show that the Ypt1-Atg11 interaction is required for PAS assembly under normal growth conditions. Moreover, we show that Trs85, Ypt1 and Atg11 function as one module and interact on Atg9-containing membranes and on PAS. These results define a module comprised of a GEF, Trs85-containing TRAPP III, a Ypt/Rab GTPase, Ypt1, and an effector, Atg11, that plays a role at the onset of autophagy. Because Ypt1 and TRAPP complexes are involved in both ER-to-Golgi and autophagy, we propose that they coordinate the divergence of these processes by recruiting process-specific effectors.

Results

Atg11 is a downstream effector of Ypt1

Atg11, which interacts with multiple Atg proteins through three of its coiled-coil domains (Figure 1A, [19]), was identified as a Ypt1 interactor in two independent yeast-two hybrid screens. We verified this interaction in both plasmid orientations (Figure 1B and C), and showed that it is specific to Ypt1, because Atg11 does not interact with Ypt6, Ypt31, or Sec4 (Figure 1B); the last two play a role in autophagy [20]. Furthermore, Atg11 interaction with Ypt1 is nucleotide specific as it interacts with the GTP, but not the GDP or nucleotide-free, form of Ypt1 (Figure 1C). Coiled-coils 2 and 3 of Atg11 are required and sufficient for the interaction with Ypt1-GTP (Figures S1 and 1B). These results suggest Atg11 as a Ypt1 effector, with the middle region of Atg11 mediating the interaction. This region is involved in multiple Atg11 interactions and is required for its function in selective autophagy [19].

To determine whether the Ypt1-Atg11 interaction occurs *in vitro*, we tested co-precipitation of HA-tagged Atg11 from yeast lysates with purified recombinant GST-Ypt1. Atg11-HA co-precipitates preferentially with GST-Ypt1 loaded with GTP, and not with GST-Ypt1-GDP or GST (Figure 1D). The low level of the co-precipitation from yeast lysates can be attributed to a transient nature of the interaction or to competition with other yeast proteins interacting with Atg11. To determine whether recombinant Ypt1 and Atg11 proteins interact, the CC2-3 domain of Atg11 (amino-acids 321-859), which interacts with Ypt1 in the yeast-two hybrid assay, was expressed in bacteria as a His6-tagged protein. Co-precipitation of His-Atg11-CC2-3 with purified Ypt1 showed that this protein interacts preferentially with Ypt1-GTP (Figure 1E), suggesting that the Ypt1-Atg11 interaction is direct.

Cells carrying the *ypt1-1* mutation, T40K, in the effector-binding domain of Ypt1, are defective in autophagy [15, 17]. Therefore, we tested whether the Ypt1-1 mutant protein is defective in the interaction with Atg11 using the three interaction assays mentioned above: yeast-two hybrid, co-precipitation with Atg11-HA from yeast lysates, and co-precipitation with bacterially expressed His-Atg11-CC2-3 (Figure 1C-E). The Ypt1-1 mutant protein is defective in the interaction with Atg11 or with Atg11-CC2-3 in all three assays when compared to the wild type Ypt1 protein.

To determine whether Ypt1 and Atg11 interact *in vivo*, we used the bimolecular fluorescence complementation (BiFC) assay. BiFC is a protein-fragment complementation assay (PCA) in which two fragments of a fluorophore tagged to two different proteins are co-expressed in cells. Fluorescence is observed only if the two proteins interact to bring the two fluorophore fragments in close enough proximity [21]. We constructed plasmids in which yeast-optimized YFP or CFP was split into N- and C-termini: the C-termini of YFP and CFP are identical (Y/CFP-C) and the N-terminal domains, YFP-N and CFP-N, determine whether the interacting complex fluoresces in the YFP or CFP channel, respectively [21]. Split YFP was used to determine the Ypt1-Atg11 interaction *in vivo*. Only in cells co-expressing YFP-N-Atg11 and Y/CFP-C-Ypt1 or Ypt1-GTP, but not Y/CFP-C-Ypt1-1, there is one dot per cell in the YFP channel (Figure 2A), suggesting that Ypt1, but not Ypt1-1, interacts with Atg11 *in vivo*.

Two pieces of evidence support the use of Ypt1-1 as a negative control in the BiFC assay. First, immuno-fluorescence microscopy shows a similar Ypt1 pattern in wild type and *ypt1-1* (Figure S2A). Second, Y/CFP-C-Ypt1-1 interacts with Trs85-CFP-N (see below, Figure 2C). The Atg11-interacting PAS protein Atg1 [18] was used to verify the specificity of BiFC. Fluorescence was seen in cells co-expressing Y/CFP-C-Atg1

and YFP-N-Atg11, but not YFP-N-Atg1 and Y/CFP-C-Ypt1 (Figure S2B). BiFC between Atg1 and Atg11, but not between Atg1 and Ypt1, provides support for the specificity of this assay and its relevance to protein interaction.

The importance of the CC2 and CC3 domains of Atg11 for its interaction with Ypt1 was confirmed using BiFC. Fluorescence was seen only in cells co-expressing Y/CFP-C-Ypt1 and YFP-N-Atg11, but not Atg11 Δ CC2 or Atg11 Δ CC3. All three YFP-N-Atg11 proteins show a BiFC interaction with Atg19 (Figure S2C), which interact with Atg11 through CC4 [19]. These results show that the CC2 and CC3 domains of Atg11 are required for its interaction with Ypt1 *in vivo*.

When combined with markers, BiFC can be used for intracellular localization of protein interactions [21]. To determine whether the Ypt1-Atg11 interaction occurs on PAS, we tested the co-localization of the Ypt1-Atg11 BiFC puncta with the PAS marker Atg8 [22] tagged with mCherry. In all cells that show both the BiFC (YFP) and mCherry puncta, the fluorescence overlaps (40/40 cells; Figure 2B). This result supports the idea that the Ypt1-Atg11 interaction occurs in PAS.

In summary, using *in vitro* and *in vivo* approaches, Atg11 was identified as a Ypt1 effector candidate. Moreover, the Ypt1-1 mutant protein, in which one residue in the effector domain is changed, is defective in the interaction with Atg11.

The Ypt1-Atg11 interaction is required for PAS assembly

Ypt/Rab GTPases exert their function by recruiting their effectors to the proper location [1]. To test whether Ypt1 regulates the localization of Atg11, the effect of the *ypt1-1* mutation, which disrupts the Ypt1-Atg11 interaction, on the localization of GFP-Atg11 was determined. As previously shown, in wild type cells GFP-Atg11 localizes to a single dot per cell, which represents PAS [18, 23]. In contrast, in *ypt1-1* mutant cells,

GFP-Atg11 is seen as multiple puncta (Figures 3A and S3A). This observation supports the idea that Atg11 is a downstream effector of Ypt1.

The effect of the *ypt1-1* mutation on two other PAS components, Atg8 and Atg1, was determined. Like GFP-Atg11, GFP-Atg8 also localizes to a single dot in wild-type cells and to multiple dots in *ypt1-1* mutant cells (Figures 3A and S3A). Co-localization of Atg11 with Atg8 in wild type and *ypt1-1* mutant cells was tested using GFP-Atg11 and mCherry-Atg8. Whereas in wild-type cells GFP-Atg11 and mCherry-Atg8 co-localize to one dot per cell, in *ypt1-1* mutant cells the multiple dots of the two proteins do not overlap (co-localization: 95% of 40 red dots in 39 wt cells, and 2.5% of 81 dots in 25 *ypt1-1* cells; Figure 3B). Appearance of Atg8 as multiple dots in several *atg* mutant cells including *atg9Δ*, [24], and of Atg11 in *atg1Δ* mutant cells [18] was previously reported. However, the nature of these dots is not clear. Atg1 is required for an early step of PAS assembly [14]. In wild type cells GFP-Atg1 localizes to a single dot, but in *ypt1-1* mutant cells it is diffuse, even though its steady-state level is unchanged (Figures 3A, S3A-B). Together these results show that PAS assembly is defective in *ypt1-1* mutant cells.

To support the idea that the inability of the Ypt1-1 mutant protein to interact with Atg11 results in a PAS assembly defect, we tested the ability of an Atg11-Ypt1-1 fusion protein to bypass the mutant defect. In most *ypt1-1* mutant cells transformed with an empty plasmid or plasmids expressing Ypt1-1 or Atg11, Atg1 is diffuse and Atg8 is seen as multiple puncta. In cells expressing the wild-type Ypt1 protein, PAS assembly is restored and Atg1 and Atg8 localize to a single dot in most cells. Importantly, in cells expressing the Atg11-Ypt1 and Atg11-Ypt1-1 fusion proteins, there is partial suppression of the PAS assembly defect (Figures 3C and S3C). Partial suppression of the *ypt1-1* PAS assembly defect by the Atg11-Ypt1-1 fusion protein should also restore

PAS function. We followed two cargo proteins whose processing depends on delivery to the vacuole through the PAS, GFP-Atg8 and Ape1 [25]. In *ypt1-1* cells transformed with empty plasmid, or plasmids expressing Ypt1-1 or Atg11, the processing of both GFP-Atg8 and Ape1 is defective. This defect is fully restored in cells expressing Ypt1, and partially restored in cells expressing one of the fusion proteins, Atg11-Ypt1 or Atg11-Ypt1-1 (Figure 3D). These observations support the idea that the Ypt1-Atg11 interaction is required for PAS assembly and function under normal growth conditions.

Interaction of Ypt1, Trs85 and Atg11 in PAS

We hypothesized that Trs85-containing TRAPP III functions together with Ypt1 and its effector Atg11 in a GEF-GTPase-effector module that regulates autophagy. Split CFP was used to determine the Trs85-Ypt1 BiFC interaction in vivo. Only in cells expressing Trs85-CFP-N and Y/CFP-C-Ypt1 or Y/CFP-C-Ypt1-1, but not Y/CFP-C-Ypt1-GTP, multiple fluorescent dots per cell are seen in the CFP channel (Figure 2C). GFP-Ypt1 localizes to multiple punta per cell [26]. Previously published studies of intracellular localization of Trs85 tagged with GFP or 3xGFP were inconclusive [17, 27]. We tagged endogenous Trs85 with yeast-optimized EGFP and demonstrated that it is functional and localizes to multiple puncta per cell (Figure S2D). Therefore, both live-cell microscopy and BiFC show that Ypt1 and Trs85 localize to and interact in more than one place in the cell. The BiFC interaction of Ypt1-1 with Trs85 shows that Ypt1-1 is not defective in the interaction with its activator. The fact that Ypt1-GTP does not show interaction with Trs85 in this BiFC assay serves as a negative control.

If the Ypt1-Trs85 interaction occurs in PAS, we expect that one of the BiFC puncta in each cell would localize to PAS. Cells expressing Trs85-CFP-N and Y/CFP-C-Ypt1 were transformed with a third plasmid expressing the PAS marker Atg8 tagged

with mCherry. In each cell that shows both CFP and red mCherry puncta, at least one blue punctum overlaps with the red punctum (25/25 cells; Figure 2D). This result indicates that the Ypt1 and Trs85 interact in PAS.

The co-localization of all three proteins, Trs85, Ypt1 and Atg11, was determined using multicolor BiFC. This assay allows simultaneous visualization of multiple protein interactions in the same cell [21]. Cells were transformed with three plasmids expressing Y/CFP-C-Ypt1, Trs85-CFP-N and YFP-N-Atg11. Fluorescence was determined in both the CFP and the YFP channels. As in the single-color BiFC described above, a few fluorescent puncta are seen in the CFP channel, showing the Ypt1-Trs85 interaction, and only one dot per cell is seen in the YFP channel, reflecting the Ypt1-Atg11 interaction. The merged images demonstrate that in each cell that shows YFP and CFP fluorescence there is a single dot in which all three proteins co-localize (in 50/50 cells with YFP and CFP fluorescence; Figure 2E). Because Atg11 is a component of PAS, and because we showed that both the Ypt1-Atg11 and the Ypt1-Trs85 BiFC puncta co-localize with the PAS marker Atg8, these results indicate that all three proteins, Ypt1, Trs85 and Atg11, co-localize and interact in PAS.

A role for the Trs85-Ypt1-Atg11 module in autophagy

To support the idea that Trs85, Ypt1 and Atg11 function as a GEF-GTPase-effector module in autophagy, we used over-expression and double-mutant analyses.

Usually, over-expression of a protein can suppress defects caused by mutant proteins that act upstream, but not downstream, in the same pathway [28]. Therefore, over-expression of Ypt1 is expected to suppress the cargo-processing defect in cells deleted for its upstream regulator Trs85, but not in cells deleted for its downstream effector Atg11. Suppression of the Ape1 processing phenotype of *trs85* Δ was shown

previously when the GTP-restricted form, but not wild type Ypt1, was expressed from the *GAL1* promoter [17]. We observed that over-expression of Ypt1 from its own promoter suppresses the Ape1 processing defect of *ypt1-1* and *trs85Δ*, but not that of *atg11Δ* (Figure 4A). This suppression is specific to Ypt1, since over-expression of Ypt31 does not suppress this defect (Figure S4A). Thus, over-expression analysis supports the idea that PAS function is regulated by a module in which Ypt1 functions downstream of Trs85 and upstream of Atg11.

If two proteins function in the same pathway, a double deletion mutant should confer a phenotype not more severe than the phenotypes of the single deletions. When grown in rich medium, the *trs85Δ*, *ypt1-1*, and *atg11Δ* mutations confer a complete block in Ape1 processing and Atg8-GFP is not processed even in wild type cells (Figure 4B and C). Therefore, we tested these plus the growth and Pho8Δ60 activity phenotypes of the mutants under nitrogen starvation. Cells carrying single deletions of *trs85Δ* and *atg11Δ* exhibit intermediate growth and Pho8Δ60 defects when compared to *ypt1-1* and *atg1Δ* cells, respectively (Figures S4B and 4D, respectively). In both assays, under nitrogen starvation *trs85Δ* confers a more severe phenotype than *atg11Δ*. These results are in agreement with the idea that Ypt1 and Trs85 play a role in both selective and non-selective autophagy [15, 17]. The observation that *atg11Δ* mutant cells also exhibit mild growth and Pho860 defects under nitrogen starvation is in agreement with the idea that PAS assembled during normal growth can persist and help cells survive under starvation conditions [29].

Because the single deletions, *trs85Δ* and *atg11Δ*, exhibit partial autophagy defects, it was possible to determine whether the double deletion phenotypes are more severe than those of the single deletions. The double mutant *trs85Δ atg11Δ* exhibits

starvation-induced growth and Pho8 Δ 60 defects similar to, and not more severe than, those of the single deletions (Figures S4B and 4D). The cargo-processing phenotypes of the single and double mutant cells were also compared under nitrogen starvation. All mutant strains exhibit varying degrees of Ape1 and Atg8 processing defects, with *ypt1-1* exhibiting the most severe defects. Importantly, the processing defects of the *atg11 Δ trs85 Δ* double deletion are not more severe than those of the single deletions (Figure 4B-C). Together, these results support the idea that the two Ypt1 interactors, Trs85 and Atg11, function in one module that regulates autophagy.

Localization of the Trs85-Ypt1 interaction to Atg9-containing membranes

As shown above, one punctum of the Trs85-Ypt1 BiFC interaction in each cell localizes to PAS (Figure 2D). To determine the localization of the rest of the Ypt1-Trs85 interaction puncta, cells expressing RFP-tagged compartmental markers [27] were transformed with plasmids co-expressing Trs85-CFP-N and Y/CFP-C-Ypt1. We did not observe obvious co-localization of the CFP and RFP fluorescence for ER exit sites, cis Golgi, Golgi, trans Golgi or endosomes (Figure S5). Thus, the bulk of the Ypt1-Trs85 interaction does not occur on exocytic or endocytic compartments. However, it is still an open question whether some interaction occurs on those compartments.

Atg9 is an integral membrane protein, and Atg9-containing membranes were proposed as a source for the autophagosome biogenesis. Like Ypt1 and Trs85, Atg9 localizes to multiple puncta per cell [30]. Partial co-localization of Ypt1 and Atg9 was recently reported [17]. To determine whether the Ypt1-Trs85 interaction occurs on Atg9-marked membranes, the Trs85-Ypt1 BiFC puncta were co-localized with Atg9-mCherry. While there are more Atg9 mCherry puncta in each cell, all the CFP puncta representing the Ypt1-Trs85 interaction co-localize with Atg9 (multiple puncta in 25/25 cells,

Figure 4E). If the BiFC puncta representing the Trs85-Ypt1 interaction sites co-localize with Atg9, we expected that Trs85 itself also co-localizes with Atg9. Like the BiFC puncta, all the Trs85 puncta overlap with Atg9 puncta (75/75 puncta in 30 cells), but there are additional Atg9 puncta in each cell (Figure S4C). This result provides a BiFC-independent confirmation for the co-localization of Trs85 with Atg9. Because Atg11 interacts with Atg9 and affects its cellular localization [23], we wished to determine whether Ypt1 or Trs85 affect this localization as well. The number of Atg9-mCherry puncta is reduced in both *trs85* Δ and *ypt1-1* mutant cells when compared to wild type cells (Figure S4D). Thus, Ypt1 and Trs85 affect the localization of Atg9, an Atg11 interactor. Together, these results suggest that Trs85 and Ypt1 interact on Atg9-containing membranes, which serve as source for the membrane on which PAS assembles. In addition, proper function of Trs85 and Ypt1 is important for Atg9 localization.

Discussion

PAS assembly is the first step of the selective and non-selective autophagy pathways, and Atg11 is a PAS organizer in selective autophagy [14]. Here we show that Atg11 is a downstream effector of Ypt1 based on the following evidence: in vitro and in vivo analyses show that Atg11 interacts specifically with the GTP-bound form of Ypt1, and the localization of Atg11 to PAS is regulated by Ypt1. Using *ypt1-1*, a mutant defective in the interaction with Atg11, we show that the Ypt1-Atg11 interaction is important for PAS assembly and function. Moreover, multi-color BiFC analysis shows that Trs85, an autophagy-specific subunit of the Ypt1 activator complex, interacts with Ypt1 on Atg9-containing membranes and with Ypt1 and Atg11 in PAS. Finally, genetic analyses support the idea that the three proteins function as a GEF-GTPase-Effector module to regulate PAS assembly (Figure 5F). To our knowledge, this is the first Ypt/Rab GTPase module reported to regulate the onset of autophagy.

Our observation that under nitrogen starvation the *ypt1-1* mutation confers more severe autophagy defects than those exhibited by *trs85Δ* and *atg11Δ* suggests that alternative Ypt1 activators and effectors function in non-selective autophagy. Atg11 and Atg17 seem to play similar roles in specific and non-specific autophagy, respectively [29], including the recruitment of Atg9 to PAS [23, 31]. Because Ypt1 is involved in both non-selective and selective autophagy and Atg11 is involved mainly in the former, Atg17 is a potential candidate for an alternative Ypt1 effector in non-selective autophagy.

Is the role of the Ypt1 module in PAS assembly conserved from yeast to human cells? Rab1 is a functional homolog of Ypt1 [8] and a role for Rab1 in autophagy was shown in mammalian cells [16]. A recent proteomic study suggests that KIAA1012, a human Trs85 homolog, plays a role in autophagy [32]. Atg11 is conserved among yeast

and fungi, and there is no clear human homologue for Atg11 [33]. However, RB1CC1/FIP200 (KIAA0203) was suggested as a candidate for a human homologue of the yeast Atg11 or Atg17 [34, 35]. In addition, like the effect of the *ypt1-1* mutation on Atg9 localization in yeast, inhibition of Rab1a function was shown to alter the localization of Atg9 in human cells [36]. Therefore, it is tempting to propose that the role of the Trs85-Ypt1-Atg11 module in autophagy is conserved.

An open question in the autophagy field is the identity of the membrane that serves as a source for autophagosomes. Using BiFC combined with co-localization analysis we show that Ypt1 and Trs85 interact on Atg9-marked membranes. Because Atg9-containing membranes are considered a source for autophagosomal membrane [14], we propose that that Ypt1 and Trs85 are recruited to these membranes to initiate PAS assembly (Figure 5F). Ypt1 shows two different BiFC patterns: multiple puncta for the Trs85-Ypt1 interaction on Atg9-containing membrane, and a single punctum of the Trs85-Ypt1-Atg11 on Atg8/Atg9-marked PAS. Because Atg9-containing reservoirs were shown to generate PAS [30], we propose that Ypt1 interacts first with Trs85 on Atg9-containing membranes, and later with Atg11 to facilitate PAS assembly (Figure 5F). Interestingly, interaction with Atg11 is required for targeting Atg9 to PAS [23], and here we show that Ypt1 also plays a role in Atg9 localization. Since one mechanism suggested for Ypt/Rab mechanism of action is enhancement of interactions between effectors and effector-binding proteins [37], it is possible that Ypt1 enhances the Atg11-Atg9 interaction.

GTPases were implicated in the coordination of vesicular transport sub-steps and in the integration of transport steps into whole pathways [38]. Here, we propose that GTPases can also coordinate two different processes. How can one GTPase, Ypt1,

function in two different processes, ER-to-Golgi and autophagy? Each Ypt/Rab GTPase can recruit multiple effectors in a timely and spatially regulated manner. We propose that two Ypt1 effectors exhibit process specificity: the conserved tethering factor Uso1/p115 acts as an effector of Ypt1/Rab1 in the ER-to-Golgi transport step [10, 11], whereas Atg11 is an autophagy-specific Ypt1 effector. Therefore, our results imply that Ypt/Rab GTPases can regulate two different processes by recruiting process-specific effectors (Figure 5F). A future challenge is to determine the cues that allow Ypt1 to recruit a specific set of effectors to a specific membrane. One example of such discrimination is a Rab5 effector that can be recruited specifically to PI(3)P membranes [39].

Materials and Methods

All Strains, plasmids and reagents, yeast culture conditions and viability, protein level, co-precipitation and ALP activity analyses, IF and live-cell microscopy are detailed in Supplementary Information. Results shown in each figure are representative of at least two independent experiments; Bar in micrographs, 5 μ M (unless otherwise specified); +/- and bars represent STDEV.

Acknowledgments: We thank C. Richardson and F. Liu for performing early experiments, A. Shah for critical reading, Y. Liang and D. Klionsky for strains, plasmids and antibodies. This research was supported by grant GM-45444 from NIH to N. Segev.

References

1. Segev, N., *Ypt and Rab GTPases: insight into functions through novel interactions*. Curr Opin Cell Biol, 2001. **13**(4): p. 500-11.
2. Segev, N., *Ypt/rab gtpases: regulators of protein trafficking*. Sci STKE, 2001. **2001**(100): p. re11.
3. Jedd, G., C. Richardson, R. Litt, and N. Segev, *The Ypt1 GTPase is essential for the first two steps of the yeast secretory pathway*. J Cell Biol, 1995. **131**(3): p. 583-90.
4. Segev, N., *Mediation of the attachment or fusion step in vesicular transport by the GTP-binding Ypt1 protein*. Science, 1991. **252**(5012): p. 1553-6.
5. Segev, N., J. Mulholland, and D. Botstein, *The yeast GTP-binding YPT1 protein and a mammalian counterpart are associated with the secretion machinery*. Cell, 1988. **52**(6): p. 915-24.
6. Jones, S., C. Newman, F. Liu, and N. Segev, *The TRAPP complex is a nucleotide exchanger for Ypt1 and Ypt31/32*. Mol Biol Cell, 2000. **11**(12): p. 4403-11.
7. Morozova, N., Y. Liang, A.A. Tokarev, S.H. Chen, R. Cox, J. Andrejic, Z. Lipatova, V.A. Sciorra, S.D. Emr, and N. Segev, *TRAPP II subunits are required for the specificity switch of a Ypt-Rab GEF*. Nat Cell Biol, 2006. **8**(11): p. 1263-9.
8. Haubruck, H., R. Prange, C. Vorgias, and D. Gallwitz, *The ras-related mouse ypt1 protein can functionally replace the YPT1 gene product in yeast*. Embo J, 1989. **8**(5): p. 1427-32.
9. Pind, S.N., C. Nuoffer, J.M. McCaffery, H. Plutner, H.W. Davidson, M.G. Farquhar, and W.E. Balch, *Rab1 and Ca²⁺ are required for the fusion of carrier vesicles mediating endoplasmic reticulum to Golgi transport*. J Cell Biol, 1994. **125**(2): p. 239-52.
10. Allan, B.B., B.D. Moyer, and W.E. Balch, *Rab1 recruitment of p115 into a cis-SNARE complex: programming budding COPII vesicles for fusion*. Science, 2000. **289**(5478): p. 444-8.
11. Cao, X., N. Ballew, and C. Barlowe, *Initial docking of ER-derived vesicles requires Usa1p and Ypt1p but is independent of SNARE proteins*. Embo J, 1998. **17**(8): p. 2156-65.
12. Rabinowitz, J.D. and E. White, *Autophagy and metabolism*. Science, 2010. **330**(6009): p. 1344-8.
13. Kraft, C., F. Reggiori, and M. Peter, *Selective types of autophagy in yeast*. Biochim Biophys Acta, 2009. **1793**(9): p. 1404-12.
14. Weidberg, H., E. Shvets, and Z. Elazar, *Biogenesis and cargo selectivity of autophagosomes*. Annu Rev Biochem, 2011. **80**: p. 125-56.
15. Segev, N. and D. Botstein, *The ras-like yeast YPT1 gene is itself essential for growth, sporulation, and starvation response*. Mol Cell Biol, 1987. **7**(7): p. 2367-77.
16. Zoppino, F.C., R.D. Militello, I. Slavin, C. Alvarez, and M.I. Colombo, *Autophagosome formation depends on the small GTPase Rab1 and functional ER exit sites*. Traffic, 2010. **11**(9): p. 1246-61.
17. Lynch-Day, M.A., D. Bhandari, S. Menon, J. Huang, H. Cai, C.R. Bartholomew, J.H. Brumell, S. Ferro-Novick, and D.J. Klionsky, *Trs85 directs a Ypt1 GEF, TRAPP III, to the phagophore to promote autophagy*. Proc Natl Acad Sci U S A, 2010. **107**(17): p. 7811-6.

18. Kim, J., Y. Kamada, P.E. Stromhaug, J. Guan, A. Hefner-Gravink, M. Baba, S.V. Scott, Y. Ohsumi, W.A. Dunn, Jr., and D.J. Klionsky, *Cvt9/Gsa9 functions in sequestering selective cytosolic cargo destined for the vacuole*. *J Cell Biol*, 2001. **153**(2): p. 381-96.
19. Yorimitsu, T. and D.J. Klionsky, *Atg11 links cargo to the vesicle-forming machinery in the cytoplasm to vacuole targeting pathway*. *Mol Biol Cell*, 2005. **16**(4): p. 1593-605.
20. Geng, J., U. Nair, K. Yasumura-Yorimitsu, and D.J. Klionsky, *Post-Golgi Sec proteins are required for autophagy in Saccharomyces cerevisiae*. *Mol Biol Cell*, 2010. **21**(13): p. 2257-69.
21. Kerppola, T.K., *Bimolecular fluorescence complementation (BiFC) analysis as a probe of protein interactions in living cells*. *Annu Rev Biophys*, 2008. **37**: p. 465-87.
22. Kim, J., W.P. Huang, and D.J. Klionsky, *Membrane recruitment of Aut7p in the autophagy and cytoplasm to vacuole targeting pathways requires Aut1p, Aut2p, and the autophagy conjugation complex*. *J Cell Biol*, 2001. **152**(1): p. 51-64.
23. He, C., H. Song, T. Yorimitsu, I. Monastyrska, W.L. Yen, J.E. Legakis, and D.J. Klionsky, *Recruitment of Atg9 to the preautophagosomal structure by Atg11 is essential for selective autophagy in budding yeast*. *J Cell Biol*, 2006. **175**(6): p. 925-35.
24. Suzuki, K., T. Kirisako, Y. Kamada, N. Mizushima, T. Noda, and Y. Ohsumi, *The pre-autophagosomal structure organized by concerted functions of APG genes is essential for autophagosome formation*. *Embo J*, 2001. **20**(21): p. 5971-81.
25. Cheong, H. and D.J. Klionsky, *Biochemical methods to monitor autophagy-related processes in yeast*. *Methods Enzymol*, 2008. **451**: p. 1-26.
26. Calero, M., C.Z. Chen, W. Zhu, N. Winand, K.A. Havas, P.M. Gilbert, C.G. Burd, and R.N. Collins, *Dual prenylation is required for Rab protein localization and function*. *Mol Biol Cell*, 2003. **14**(5): p. 1852-67.
27. Huh, W.K., J.V. Falvo, L.C. Gerke, A.S. Carroll, R.W. Howson, J.S. Weissman, and E.K. O'Shea, *Global analysis of protein localization in budding yeast*. *Nature*, 2003. **425**(6959): p. 686-91.
28. Jones, S., G. Jedd, R.A. Kahn, A. Franzusoff, F. Bartolini, and N. Segev, *Genetic interactions in yeast between Ypt GTPases and Arf guanine nucleotide exchangers*. *Genetics*, 1999. **152**(4): p. 1543-56.
29. Cheong, H., U. Nair, J. Geng, and D.J. Klionsky, *The Atg1 kinase complex is involved in the regulation of protein recruitment to initiate sequestering vesicle formation for nonspecific autophagy in Saccharomyces cerevisiae*. *Mol Biol Cell*, 2008. **19**(2): p. 668-81.
30. Mari, M., J. Griffith, E. Rieter, L. Krishnappa, D.J. Klionsky, and F. Reggiori, *An Atg9-containing compartment that functions in the early steps of autophagosome biogenesis*. *J Cell Biol*, 2010. **190**(6): p. 1005-22.
31. Sekito, T., T. Kawamata, R. Ichikawa, K. Suzuki, and Y. Ohsumi, *Atg17 recruits Atg9 to organize the pre-autophagosomal structure*. *Genes Cells*, 2009. **14**(5): p. 525-38.
32. Behrends, C., M.E. Sowa, S.P. Gygi, and J.W. Harper, *Network organization of the human autophagy system*. *Nature*, 2010. **466**(7302): p. 68-76.
33. Meijer, W.H., I.J. van der Klei, M. Veenhuis, and J.A. Kiel, *ATG genes involved in non-selective autophagy are conserved from yeast to man, but the selective Cvt and pexophagy pathways also require organism-specific genes*. *Autophagy*, 2007. **3**(2): p. 106-16.

34. Hara, T., A. Takamura, C. Kishi, S. Iemura, T. Natsume, J.L. Guan, and N. Mizushima, *FIP200, a ULK-interacting protein, is required for autophagosome formation in mammalian cells*. J Cell Biol, 2008. **181**(3): p. 497-510.
35. Ohashi, Y. and S. Munro, *Membrane delivery to the yeast autophagosome from the Golgi-endosomal system*. Mol Biol Cell, 2010. **21**(22): p. 3998-4008.
36. Winslow, A.R., C.W. Chen, S. Corrochano, A. Acevedo-Arozena, D.E. Gordon, A.A. Peden, M. Lichtenberg, F.M. Menzies, B. Ravikumar, S. Imarisio, S. Brown, C.J. O'Kane, and D.C. Rubinsztein, *alpha-Synuclein impairs macroautophagy: implications for Parkinson's disease*. J Cell Biol, 2010. **190**(6): p. 1023-37.
37. Segev, N., *Cell biology. A TIP about Rabs*. Science, 2001. **292**(5520): p. 1313-4.
38. Segev, N., *Coordination of intracellular transport steps by GTPases*. Semin Cell Dev Biol, 2011. **22**(1): p. 33-8.
39. Simonsen, A., R. Lippe, S. Christoforidis, J.M. Gaullier, A. Brech, J. Callaghan, B.H. Toh, C. Murphy, M. Zerial, and H. Stenmark, *EEA1 links PI(3)K function to Rab5 regulation of endosome fusion*. Nature, 1998. **394**(6692): p. 494-8.

Figure Legends

Figure 1. Atg11 is a Ypt1 effector. **A.** Schematic diagram of Atg11, its coiled-coil domains (CC) and interactors. CC2-4 positioning is based on COILS (CC1 was suggested in [19]), interactions shown under CC2-4 were previously reported [19, 23], interaction with Ypt1 is reported here. **B.** Interaction of Ypt1, but not other Ypts, with Atg11 in the yeast-two hybrid (Y2H) assay. Interaction of Atg11 and Atg11-CC2-3 with the GTP-restricted forms of the Ypts (Ypt1-Q67L, Ypt6-Q69L, Ypt31-Q72L, Sec4-Q79L) was determined. **C.** The Y2H interaction of Ypt1 with Atg11 is nucleotide specific. Only the wild type (Ypt1) and Ypt1-GTP (Q67L) interact with Atg11, whereas Ypt1-GDP (S22N), the nucleotide-free form (Ypt1-NF, D124N) and Ypt1-1 (T40K) do not. Immunoblot analysis shows expression of the different Ypt proteins (B-C, bottom). **D.** Atg11-HA from yeast cell lysates co-precipitates with purified Ypt1-GTP, but not with Ypt1-GDP or Ypt1-1 mutant protein (GTP or GDP). Atg11-HA (top, left lane, 10% of lysate) co-precipitated preferentially with GST-Ypt1 loaded with GTP (T) (0.49 +/- 0.02 % of lysate above the background), and not with GST-Ypt1 loaded with GDP (D), GST-Ypt1-1 loaded with GTP or GDP, or GST (Φ). **E.** Interaction of recombinant Ypt1, but not Ypt1-1, with Atg11-CC2-3. The experiment was done as described in panel D, except that co-precipitation was done with bacterial lysates expressing His6-tagged Atg11-CC2-3 (left lane, 10% loaded). His6-Atg11-CC2-3 co-precipitates preferentially with GST-Ypt1-GTP, and not with GST-Ypt1-GDP, GST-Ypt1-1 GDP or GTP, or GST (Φ). The level of precipitated GST-tagged proteins is shown at the bottom of panels D and E.

Figure 2. PCA for Ypt1, Atg11 and Trs85 using multicolor BiFC. **A.** Positive PCA for Atg11 with Ypt1 and Ypt1-GTP (Ypt1-Q67L), but not with Ypt1-1. YFP fluorescence

is seen in cells co-expressing YFP-N-Atg11 with C/YFP-C-Ypt1 or Ypt1-GTP, but not C/YFP-C-Ypt1-1. No fluorescence is seen in the CFP channel. **B.** Atg11 and Ypt1 interact in Atg8-marked PAS. The experiment was done as described in panel A except that cells also express mCherry-Atg8. Overlap of YFP and mCherry fluorescence (merge) indicates that Atg11 and Ypt1 interact on PAS (arrows). **C.** Positive PCA for Trs85 with Ypt1 and Ypt1-1, but not Ypt1-GTP. CFP fluorescence is seen in cells co-expressing Trs85-CFP-N with C/YFP-C-Ypt1 (arrowheads) or C/YFP-C-Ypt1-1, but not C/YFP-C-Ypt1-GTP. No fluorescence is seen in the YFP channel. **D.** Trs85 and Ypt1 interact in Atg8-marked PAS. The experiment was done as described in panel C except that cells also express mCherry-Atg8. At least one CFP puncta per cell overlaps with mCherry (merge) indicating Trs85-Ypt1 interaction on PAS (arrows), while the rest do not (arrowheads). **E.** Multicolor BiFC of Trs85, Ypt1, and Atg11. Cells co-express Trs85-CFP-N, YFP-N-Atg11, and C/YFP-C-Ypt1. Fluorescence in the CFP channel shows the Ypt1-Trs85 interaction, YFP shows the Ypt1-Atg11 interaction, and overlap of the Ypt1-Trs85 and Ypt1-Atg11 interactions is shown in merge. Arrows point to puncta where all three proteins are present, whereas arrowheads point to dots where Ypt1 interacts with Trs85, but not with Atg11. Immuno-blot shows similar Ypt1 protein levels (A and C, bottom).

Figure 3. Ypt1 interaction with Atg11 is required for PAS assembly. **A.** The localization of three GFP-tagged PAS components, Atg11, Atg8 and Atg1, is altered in *ypt1-1* mutant cells. In wild type cells each of the three proteins localizes to one dot, whereas in *ypt1-1* cells Atg11 and Atg8 localize to multiple puncta and Atg1 is diffuse. (quantification, Figure S3A; protein level, Figure S3B). **B.** GFP-Atg11 and mCherry-Atg8 do not co-localize in *ypt1-1* cells. In wild type cells Atg11 and Atg8 co-localize in one

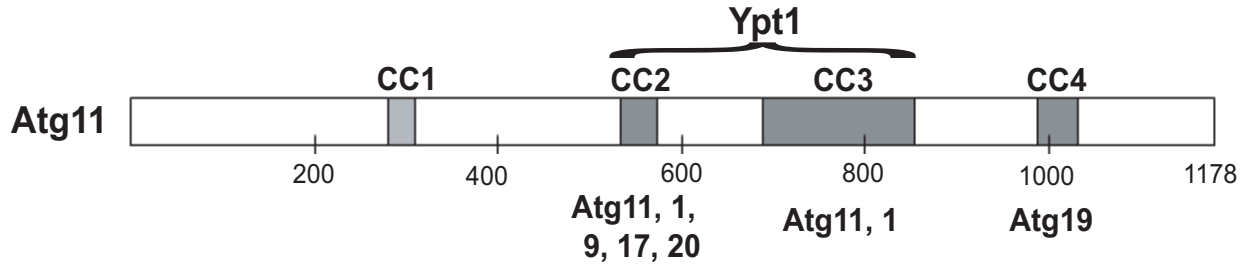
dot, while in *ypt1-1* cells, the multiple puncta of Atg11 and Atg8 do not co-localize. Bar, 1 μ M. **C.** The Atg11-Ypt1-1 fusion protein can partially restore PAS formation in *ypt1-1* cells. Like *ypt1-1* cells (Φ), cells expressing Ypt1-1 or Atg11, exhibit diffuse Atg1 and multiple puncta of Atg8. The *ypt1-1* Atg-localization defects are fully suppressed by Ypt1, and partial suppressed by one of the fusion proteins, Atg11-Ypt1 or Atg11-Ypt1-1 (quantification, Figure S3C). **D.** The Ypt1-1-Atg11 fusion protein partially suppress the maturation defects of GFP-Atg8 and Ape1 in *ypt1-1* cells. The pre-mature forms of GFP-Atg8 and Ape1 (pApe1) are present in all cells. As in *ypt1-1* cells (Φ), in cells expressing Ypt1-1 or Atg11, there is no GFP (processed from GFP-Atg8) or mature Ape1 (mApe1). These processing defects are fully suppressed by Ypt1 and partially suppressed by Atg11-Ypt1-1 or Atg11-Ypt1 (bottom, right: quantification of Ape1 maturation; bottom, left: Ypt1 and Ypt1-1 protein level).

Figure 4. A role for the Trs85-Ypt1-Atg11 module in autophagy. A. Over-expression of Ypt1 suppresses the Ape1 processing defects of *ypt1-1* and *trs85 Δ* , but not of *atg11 Δ* . All three mutants exhibit an Ape1 processing defect (accumulate the pApe1). Appearance of mApe1 is seen in *ypt1-1* and *trs85 Δ* , but not *atg11 Δ* , over-expressing Ypt1. **B.** The Ape1 processing defect of *atg11 Δ trs85 Δ* double mutant under nitrogen starvation is not more severe than that of the single deletions. All mutants exhibit a complete Ape1 processing defect during normal growth (+N₂). Under nitrogen starvation (-N₂, 4 Hours), Ape1 is processed to the mature form in wild-type cells, whereas in *ypt1-1* mutant cells it stays unprocessed. *Atg11 Δ* and *atg11 Δ trs85 Δ* exhibit a partial processing defect; *trs85 Δ* exhibits a less severe defect (bottom: % mApe1). **C.** The Atg8 processing defect of *atg11 Δ trs85 Δ* double mutant under nitrogen starvation is not more severe than that of the single deletions. All strains do not process Atg8 during normal

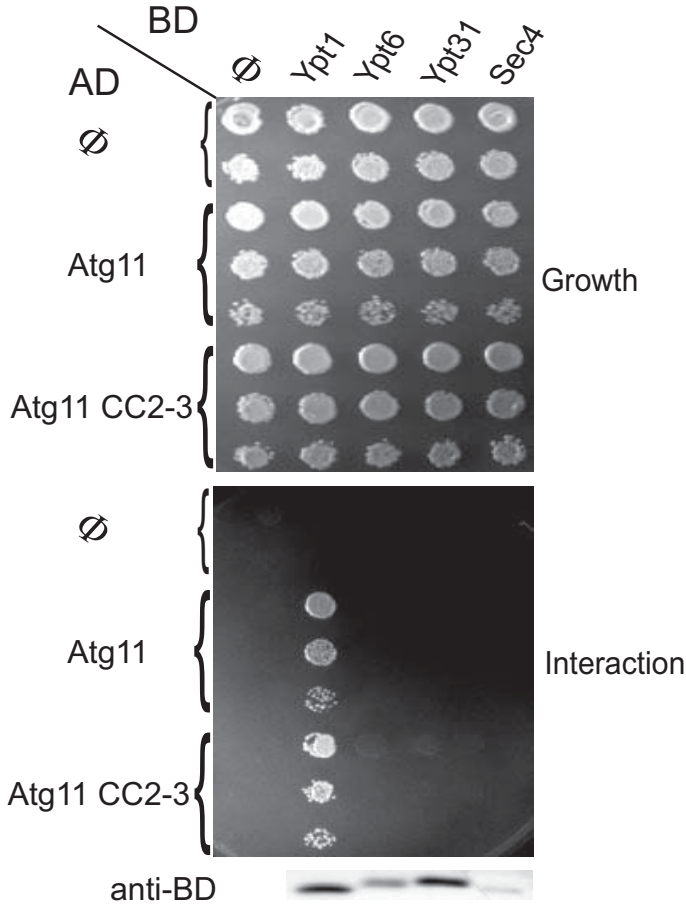
growth. Under nitrogen starvation (4 hours), most of the Atg8-GFP protein in wild-type cells is processed to GFP, whereas in *ypt1-1* mutant cells it stays as Atg8-GFP. *Trs85Δ* and *atg11Δtrs85Δ* exhibit a similar processing defect, less severe than that of *ypt1-1*; *atg11Δ* exhibits a less severe defect. **D.** The Pho8 Δ 60 ALP activity defect of *atg11Δtrs85Δ* is not more severe than in single deletions. ALP activity was determined in lysates prepared from cells grown in YPD (white bars) and after 6 hours of nitrogen starvation (gray bars); *atg1Δ* mutant cells serve as a negative control. *Trs85Δ* and *atg11Δtrs85Δ* mutant cells exhibit a similar partial defect; *atg11Δ* mutant cells exhibit a less severe defect. Units represent nmole nitrophenol/mg protein. **E.** The Trs85 and Ypt1 BiFC puncta overlap with Atg9. The experiment was done as in Figure 2D, except that Atg9 was tagged on the chromosome with mCherry. All the CFP puncta overlap with mCherry (merge), indicating that Trs85 and Ypt1 interact on Atg9-marked compartments (arrows). There are more Atg9 than Ypt1-Trs85 puncta (arrow heads). **F.** A model of how one Ypt/Rab GTPase, Ypt1, regulates two processes, ER-to-Golgi transport (top) and PAS assembly (bottom), by recruiting process-specific effectors. In ER-to-Golgi transport, Ypt1 activated by TRAPP I [6, 7] recruits the conserved tethering factor Uso1/p115 [10, 11] to stimulate ER vesicle tethering to the Golgi. In selective autophagy, a GEF-GTPase-effector module, composed of Trs85-containing TRAPP III-Ypt1-Atg11, respectively, regulates the first step of both selective and non-selective autophagy, PAS assembly. We propose that Trs85, in the context of TRAPP III, and Ypt1 are localized to Atg9-containing membranes. Subsequently, activated Ypt1-GTP, interacts with Atg11 to mediate PAS assembly on these membranes.

Figure 1

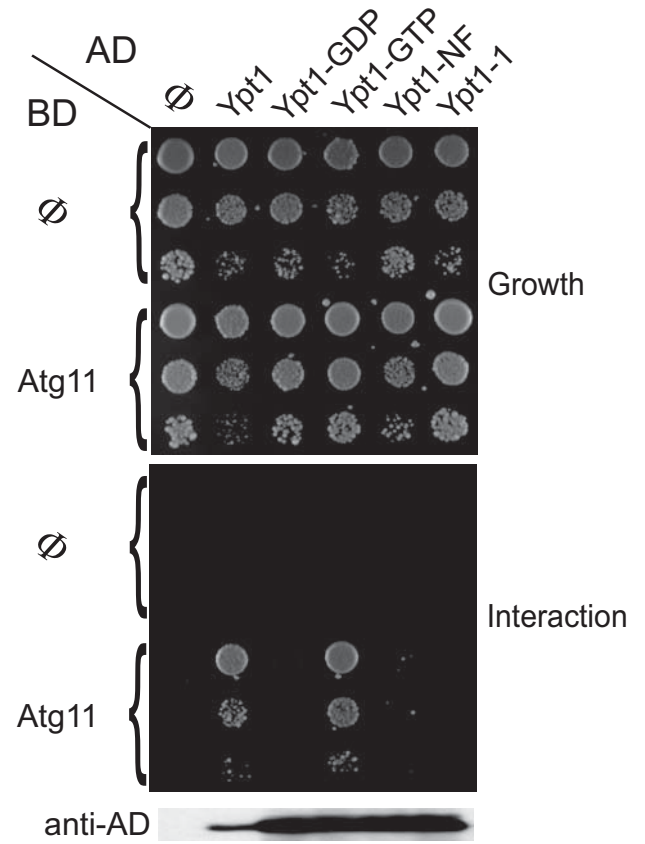
A.



B.



C.



D.



E.

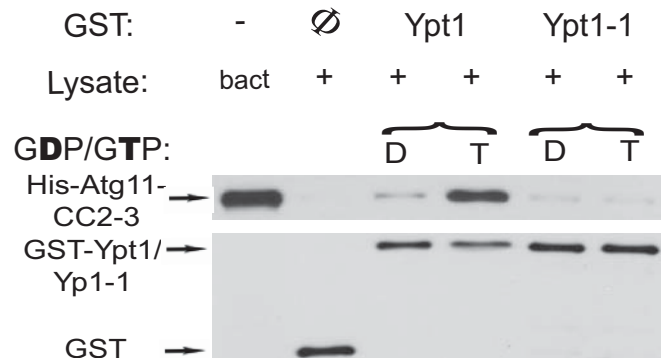
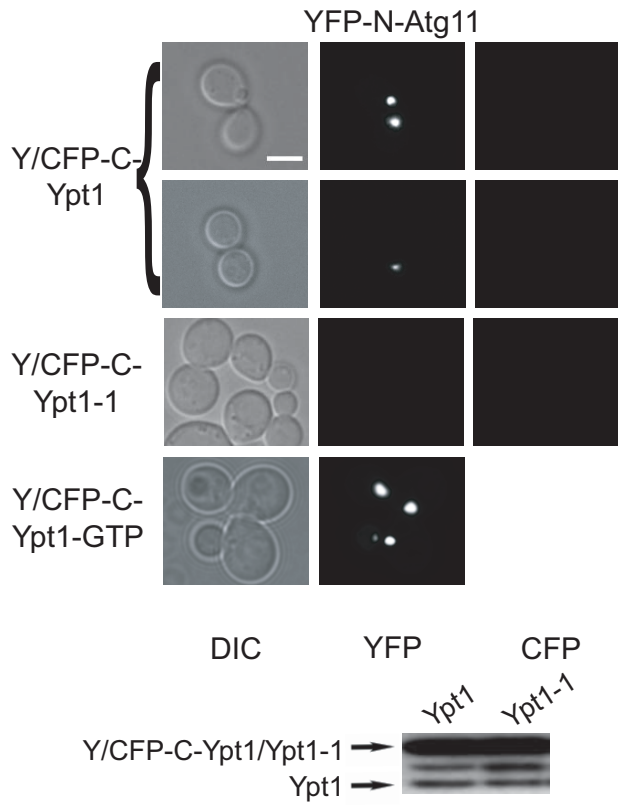
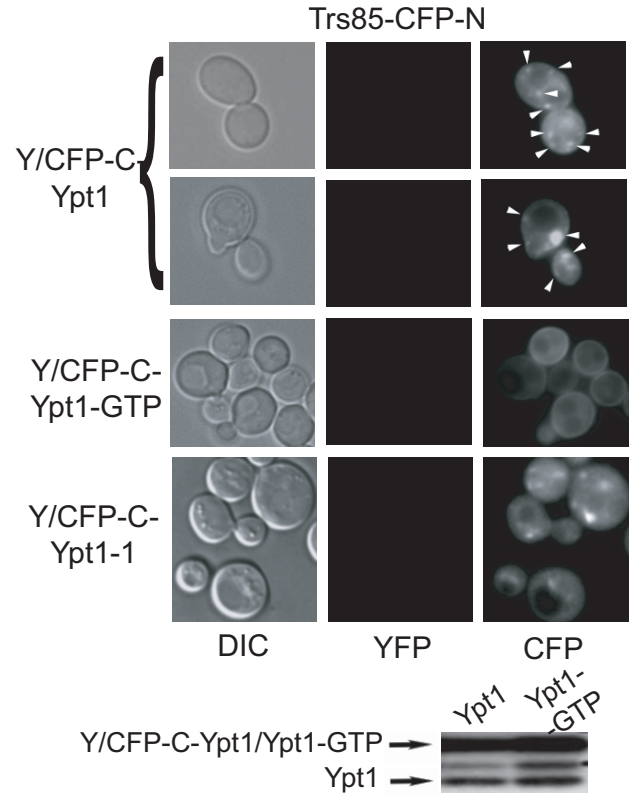


Figure 2

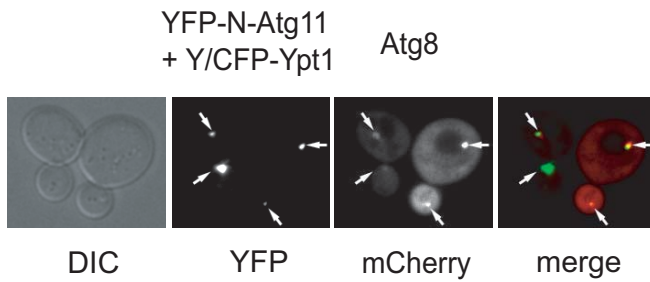
A.



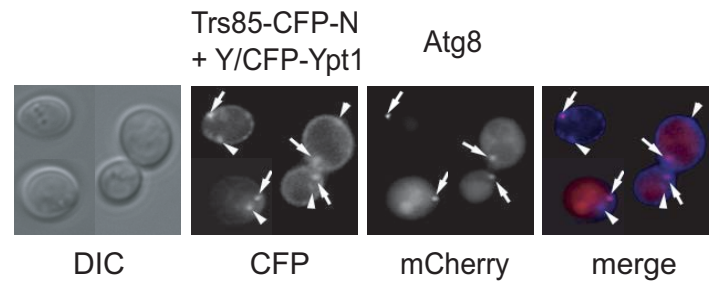
C.



B.



D.



E.

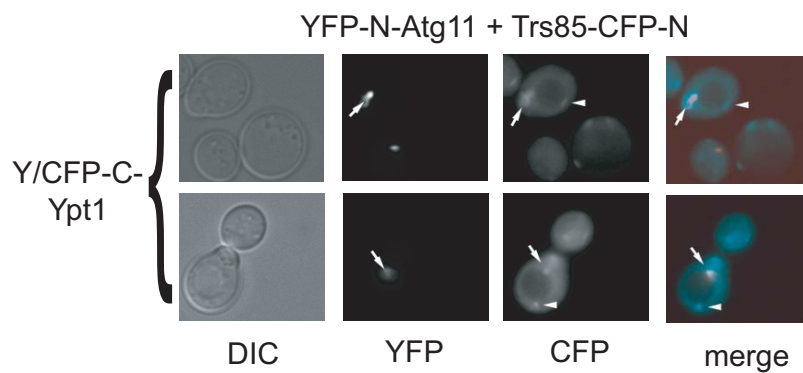


Figure 3

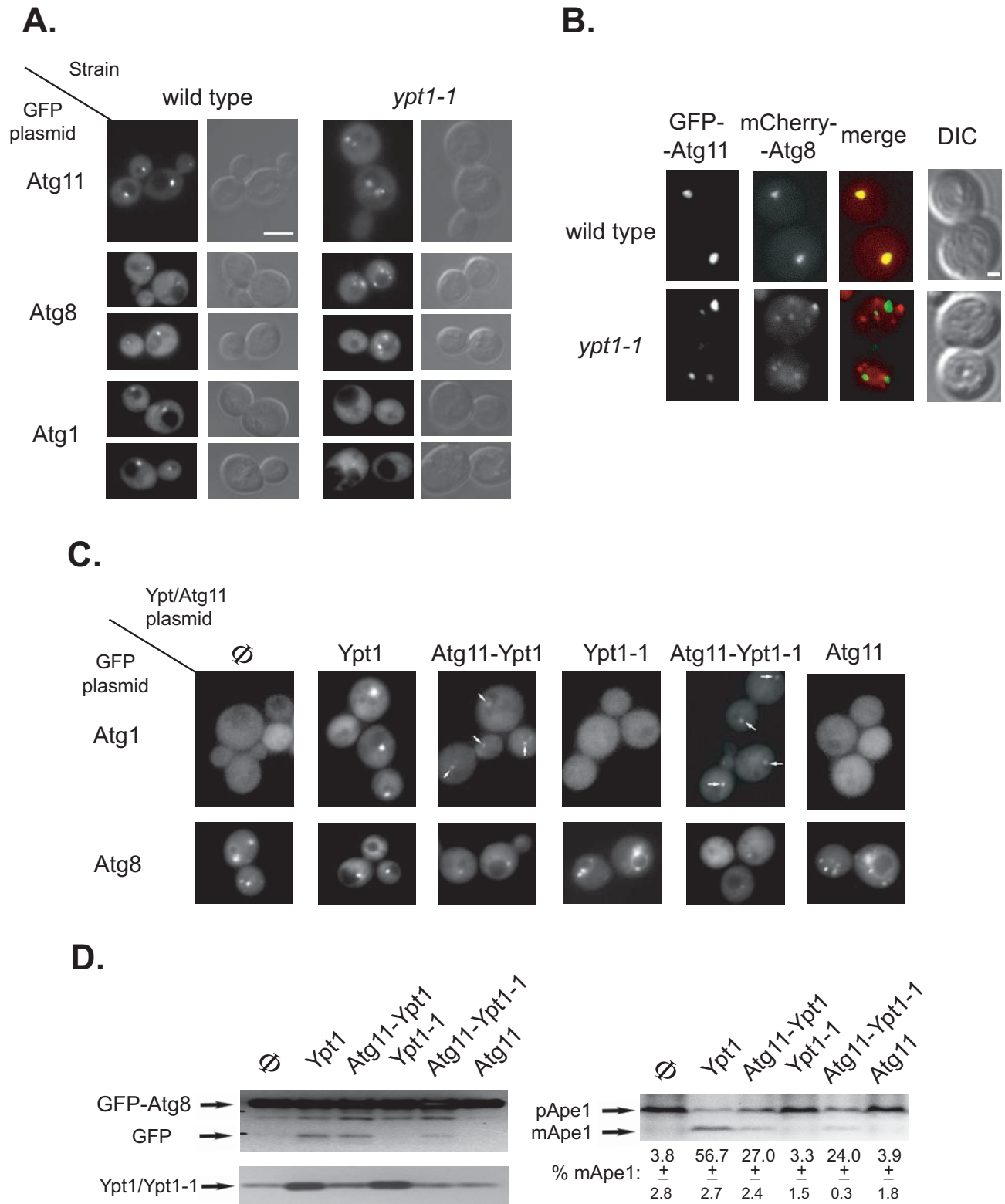
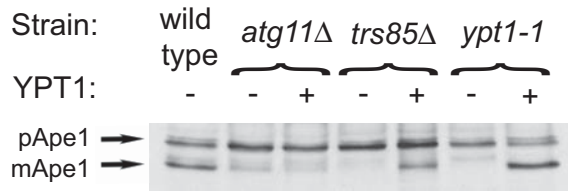
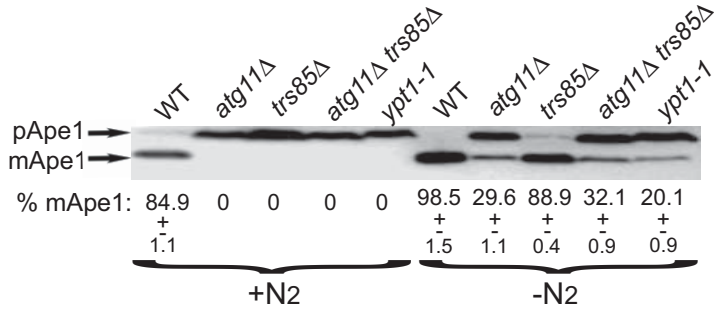


Figure 4

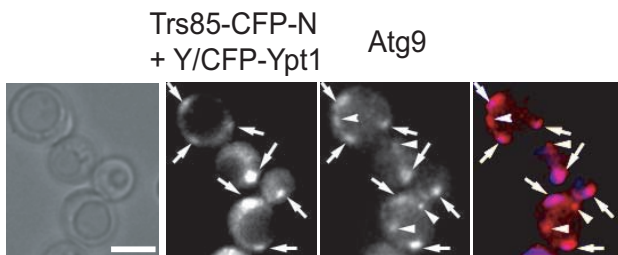
A.



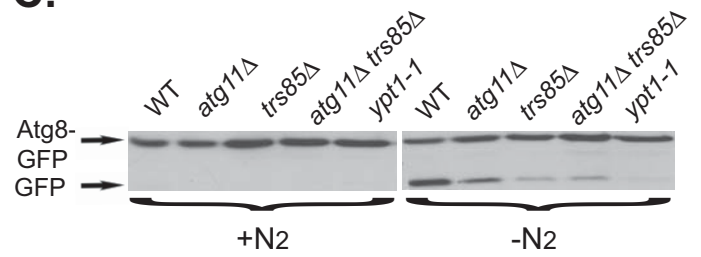
B.



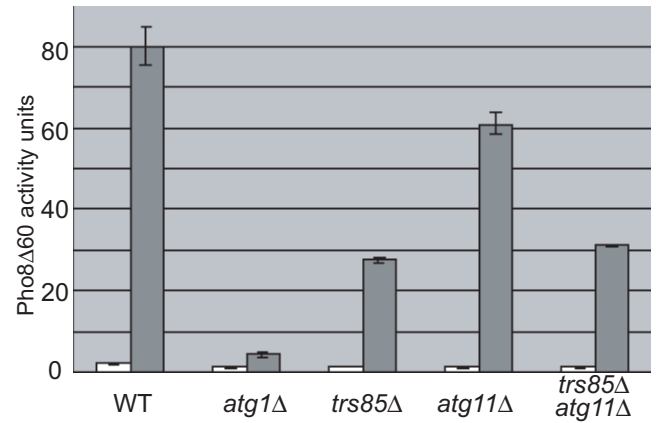
E.



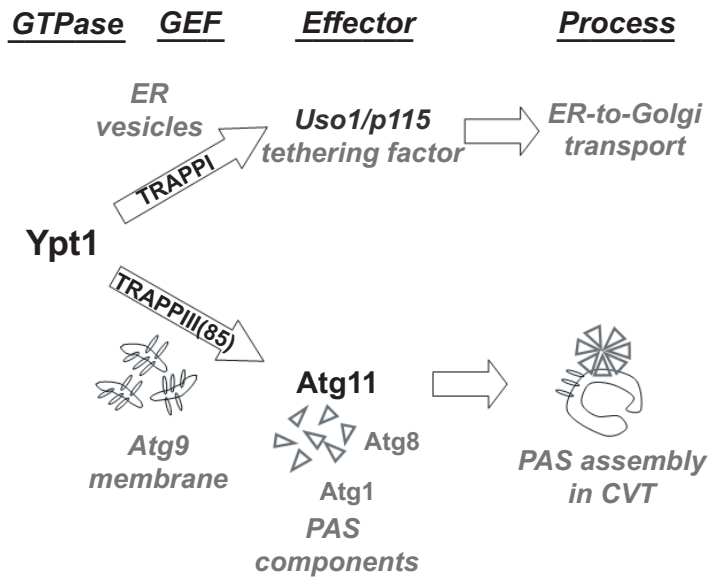
C.



D.



F.



Supplemental Material

Lipatova et al.

Supplementary Materials and Methods

Strains, plasmids and reagents

Strains used in this paper are summarized in Table S1. Yeast Strain Construction: *ATG11* was tagged on the chromosome with 3xHA at the COOH-terminus in NSY125 strain as described previously [13]. Gene deletions were done as previously described [14]. *TRS85* was tagged on the chromosome with yEGFP and *ATG9* was tagged on the chromosome with mCherry at their COOH-terminus in relevant strains as described previously [15].

Plasmids used in this study are summarized in Table S2. Plasmid Construction: For recombinant protein interaction experiments, the Atg11 CC2-3 (aa 626 - 859) peptide was cloned into the MCS1 of pCDFDuet-1 (EMD Chemicals, NJ, USA) in frame with 6xHis tag. Fusion proteins: To create Atg11-Ypt1/Ypt1-1 fusion constructs, the *Clal* – *BamHI* genomic DNA fragment containing *YPT1* ORF was cloned into pRS315. *NdeI* site was introduced right upstream of *YPT1* ORF by site-directed mutagenesis. This plasmid was used to introduce T40K mutation. *ATG11* ORF plus the AASS linker was cloned into the *NdeI* site, resulting in pRS315-Atg11-Ypt1/Ypt1-1 constructs. These were later subcloned into pRS317 using *NotI* and *Sall/PspXI* restriction sites. To make *ATG11* expressed under the control of *YPT1* promoter, we replaced *PstI* fragment of pRS315-Atg11-Ypt1 with the *PstI* fragment from pGBDU-C2-*ATG11*

thus putting a stop codon after *ATG11* ORF and removing first 65 aa of Ypt1 from the construct as well.

Plasmids used in live-cell microscopy: To construct the yEGFP-tagged versions of Atg11, Atg8, and Atg1 expressed under *ADH1* promoter, we first replaced VF1 coding fragment in p416-VF1 [10] with yEGFP amplified from pKT127 (received from EUROSCARF, [16]) using BstXI and BspEI sites, then used the obtained construct to clone the appropriate protein coding sequence in frame with yEGFP. To make the mcherry-Atg8 chimera expressed under *ADH1* promoter, we started with replacing VF1 coding fragment in p416-VF1 with mCherry amplified from pBS34 (obtained from Yeast Resource Center, [7]) using XbaI and BspEI sites, then cloned ATG8 in frame with mCherry. Later the whole fragment including *ADH1* promoter, mCherry, ATG8, and *CYC1* terminator was subcloned into pRS41H [17] using SacI and KpnI sites.

Plasmids used in BiFC: The constructs used for multicolor BiFC include NH₂-terminus of yEVENUS (172 aa) – Atg11, Trs85-NH₂ terminus of Cerulean (172 aa), and COOH-terminus of yECFP (aa 155-238) – Ypt1/ypt1-1/ypt1Q67L. All the constructs were expressed under the control of *ADH1* promoter and *CYC1* terminator, and included either a GGGG (Atg11 and Ypt1/ypt1-1/ypt1Q67L) or a GGGS (Trs85) linker. The plasmids carrying the constructs were pRS416, pRS415, and pRS413, respectively. The fragment length was selected in accordance with what was previously published [18]. To make an expression constructs for YFP-N-Atg11, YFP-N-Atg1, YFP-N-Atg11ΔCC2, and YFP-N-Atg11ΔCC3 chimeras, first the VF1 coding fragment in p416-VF1 was replaced

by the fragment encoding 172 NH₂-terminal aa of yEVENUS amplified from pKT103 (received from EUROSCARF, [16]) using SpeI/XbaI and BspEI sites, then ATG11 or ATG1 were cloned downstream and in frame with this fragment, or ATG11 Δ CC2 and ATG11 Δ CC3 were sub-cloned from pNS1387 and 1388, respectively. For Trs85-CFP-N chimera, we started with cloning the fragment encoding 172 aa of Cerulean amplified from pBS10 (obtained from Yeast Resource Center, [6]) into p415-VF2 [10] instead of VF2 using BspEI and XhoI sites, followed by cloning TRS85 without the stop codon upstream. For construction of Y/CFP-C-tagged Ypt1, ypt1-1, ypt1Q67L and Y/CFP-C-Atg1: the fragment encoding aa 155-238 of yECFP amplified from pKT102 (received from EUROSCARF, [16]) was inserted into p416-VF1 using SpeI/XbaI and BspEI restriction sites and replacing VF1, then the piece containing ADH1 promoter, aa 155-238 of yECFP, and CYC1 terminator was subcloned into pRS413 using PvuII; and finally Ypt1, ypt1-1, ypt1Q67L or Atg1 were cloned downstream of and in frame with aa 155-238 of yECFP. For Atg19-Y/CFP-C construct, ATG19 was cloned into p415-VF2.

All chemical reagents were purchased from Fisher Scientific (NJ, USA), except for the following: Media components, other than amino acids, were purchased from US Biological (MA, USA); ProtoGel for western blots from National Diagnostics (GA, USA); amino Acids, GDP and GTP γ S, p-nitrophenyl phosphate and protease inhibitors from Sigma-Aldrich; Glutathione SepharoseTM 4B beads from Amersham Biosciences (NJ, USA); EDTA-free protease inhibitor cocktail (PIC) from Roche Diagnostics (Indianapolis, IN); glass beads from

BioSpec Products (Bartlesville, OK); restriction enzymes and buffers from New England Biolabs (MA, USA); Isopropil-beta-D-thiogalactopyranoside (IPTG) from ACROS Organics (NJ, USA); and Dithiothreitol (DTT) from Invitrogen.

Antibodies used in this study included rabbit anti-GAL4-AD, rabbit anti GAL4-BD, mouse monoclonal anti-GFP (Santa Cruz Biotechnology, CA, USA); mouse monoclonal anti-HA (Covance, WI, USA); rabbit anti-glucose-6-phosphate dehydrogenase (G-6-PDH, Sigma-Aldrich, MO, USA), rabbit anti-GST (Molecular probes, OR, USA), mouse monoclonal anti-HIS (R&D Systems, MN, USA); goat anti-rabbit-HRP and goat anti-mouse-HRP (GE healthcare, UK); anti-Apel [73]; and affinity purified rabbit anti-Ypt1 [7].

Yeast culture conditions and viability analysis

For yeast two-hybrid assays haploid cells were transformed with the relevant activation domain (pACT2, AD) and binding domain (pGBDU-C2, BD) plasmids and mated. Diploid cultures were grown overnight at 26°C in minimal (SD) media, normalized to the same density by OD₆₀₀, and spotted onto agar plates in serial dilutions. Plates for yeast two-hybrid assay, indicated in figure legends, were incubated at 26°C. Media preparation and yeast culture growth for nitrogen starvation shift experiments were done as described [33]. Growth of the diploids is shown on SD-Ura-Leu plates, whereas interaction is on SD-Ura-Leu-His plates; one or two ten-fold dilutions are shown from top to bottom. Empty AD and BD plasmids (Φ) serve as negative controls for interaction.

Protein level analyses

To determine the expression level of yeast two-hybrid constructs, 4.5 OD_{600s} of overnight cell culture were spun down, resuspended in 100 µl of Laemmli buffer, boiled, vortexed with equal volume of glass beads and subjected to immuno-blot analysis with anti-GAL4-AD, anti-HA, or anti-GAL4-BD. To check the level of GFP-tagged proteins or fusion constructs, 7 OD_{600s} of exponentially growing cell cultures were spun down, resuspended in 100 µl of Laemmli buffer, boiled, vortexed with equal volume of glass beads and subjected to Western blot analysis with anti-GFP or anti-Ypt1. Preparation of yeast lysates for Ape1 and Atg8-GFP processing analysis was done as described [52]. Quantification of bands was done using ImageJ.

Co-precipitation analyses

Preparation of proteins for co-precipitation: Bacterially expressed GST-Ypt1, GST-Ypt1-1 or GST (as a negative control) proteins were expressed from pGEX-KT and purified as previously described [74]. GST-tagged proteins were purified on glutathione agarose beads and loaded with GDP (D) or GTP (T). The beads were incubated with lysates from yeast cells expressing full-length Atg11-3xHA or from bacterial cells expressing His6-tagged Atg11-CC2-3. To prepare lysates from yeast cells expressing Atg11-3xHA, 200 OD_{600s} of cells were spun down, washed twice with ice-cold water, resuspended in 10 ml of buffer containing 100 mM Tris-HCl, pH 9.4, 20m M DTT, and incubated for 15 min at 30°C. Then cells were spun down, resuspended in 4 ml oxaliticase buffer (1 M sorbitol, 50 mM Na₂PO₄, pH 7,4, 0.05 mg/ml oxaliticase) and spheroplasted for 30 min at 30°C with gentle mixing. Spheroplasts were pelleted by centrifugation

at 4000 g for 5 min and gently resuspended in 3 ml of ice-cold lysis buffer (20 mM HEPES, pH 6.8, 150 mM KOAc, 4 mM MgOAc, 250 mM Sorbitol, 0.2 % Triton X-100, 1 mM PMSF, Protease inhibitor cocktail (Complete)). Protein lysate was aliquoted and stored at -80°C. To prepare recombinant His-Atg11 CC2-3, BL21 cells were transformed with pCDF-Duet-1-Atg11 CC2-3, induced with 0.4 mM IPTG at OD 0.6-0.8 for 4 hours, collected by centrifugation, resuspended in lysis buffer (50 mM PBS, pH 7.5, 1 mM PMSF, 0.5% Triton X-100) and lysed by sonication.

Co-precipitation of Atg11-3XHA or His-Atg11 CC2-3 with GST-Ypt1 or GST-Ypt1-1 was done as previously described [16], using GTP- γ -S instead of GTP. After precipitation, the level of GST, GST-Ypt1 and GST-Ypt1-1 was determined by immuno-blot analysis using anti-GST antibody, and the level of Atg11-HA or His6-tagged Atg11-CC2-3 that co-precipitated with the GST-tagged proteins was determined using anti-HA or anti-His6 antibodies, respectively.

ALP activity assay

Alkaline phosphatase activity assay of Pho8 Δ 60 was done as previously described [75].

Microscopy

Live cell microscopy was done as follows: Wild type (NSY125) and *ypt1-1* mutant (NSY2) cells carrying constructs for GFP- or mCherry-tagged protein expression were grown to mid-log phase in appropriate selective media. Fluorescence microscopy was carried out using deconvolution Axioscope microscope (Carl Zeiss, Thornwood, NY) with FITC (GFP) and TexasRed

(mCherry) sets of filters. To visualize protein interactions in BiFC and multicolor BiFC assays, cells (NSY128) carrying the appropriate expression constructs were grown to mid-log phase in appropriate selective media and visualized using deconvolution Axioscope microscope with the filters optimized for the visualization of YFP and CFP [45]. Immuno-fluorescence microscopy using affinity-purified anti-Ypt1 antibodies was done as previously described [7].

Table S1. Yeast strains used in this study

| Strain | Alias | Genotype | Source |
|---------------|----------------------------------|---|---------------|
| NSY468 | PJ69-4A | <i>MATa trp1-901 leu2-3,112 ura3-52 his3-200 gal4Δ gal80Δ GAL2-ADE2 LYS2::GAL1-HIS3 met2::GAL7-lacZ</i> | [1] |
| NSY752 | PJ69-4α | <i>MATα trp1-901 leu2-3,112 ura3-52 his3-200 gal4Δ gal80Δ gal2-ade2 lys2::gal1-his3 met2::gal7-lacZ</i> | [1] |
| NSY125 | DBY1034 | <i>MATa his4-539 lys2-801 ura3-52</i> | [2] |
| NSY2 | <i>ypt1-1</i> (DBY1803) | <i>MATa his4-539 lys2-801 ura3-52 ypt1-T40K</i> | [3] |
| NSY128 | DBY4975 | <i>Matα ade2 his3Δ200 leu2-3,112 lys2-801 urs3-52</i> | D. Botstein |
| NSY825 | BY4741 | <i>MATa leu2Δ0 ura3Δ0 his3Δ1met15Δ0</i> | [4] |
| NSY1440 | <i>trs85Δ</i> | NSY825 <i>TRS85Δ::HYGRO</i> | This study |
| NSY1499 | <i>atg11Δ</i> | NSY825 <i>ATG11Δ::KAN</i> | This study |
| NSY1500 | <i>trs85Δ atg11Δ</i> | NSY825 <i>ATG11Δ::KAN TRS85Δ::HYGRO</i> | This study |
| NSY1508 | <i>ATG11-3xHA</i> | NSY125 <i>ATG11-3xHA::KAN</i> | This study |
| NSY1524 | <i>TRS85-yEGFP</i> | NSY825 <i>TRS85-yEGFP::KAN</i> | This study |
| NSY1523 | <i>ATG9-mCherry</i> | NSY825 <i>ATG9-mCherry::HYGRO</i> | This study |
| NSY1525 | <i>TRS85-yEGFP, ATG9-mCherry</i> | NSY825 <i>TRS85-yEGFP::KAN ATG9-mCherry::HYGRO</i> | This study |
| NSY1526 | <i>trs85Δ ATG9-mCherry</i> | NSY825 <i>TRS85Δ::KAN ATG9-mCherry::HYGRO</i> | This study |
| NSY1527 | <i>ypt1-1 ATG9-mCherry</i> | NSY55 (<i>MAα his3-200 ura3-52 leu2-3,112 ypt1-T40K</i>) <i>ATG9-mCherry::KAN</i> | This study |
| NSY1528 | <i>TN124</i> | <i>MATa leu2-3,112 trp1 ura3-52 pho8::pho8Δ60 pho13::LEU2</i> | [5] |
| NSY1529 | <i>atg1Δ in TN124</i> | NSY1528 <i>ATG1Δ::KAN</i> | Y. Liang |
| NSY1530 | <i>TN124 trs85Δ</i> | NSY <i>TRS85Δ::HYGRO</i> | This study |
| NSY1531 | <i>TN124 atg11Δ</i> | NSY <i>ATG11Δ::KAN</i> | This study |

| | | | |
|---------|--------------------------------------|-------------------------------|------------|
| NSY1532 | <i>TN124 trs85Δ</i> <i>atg11Δ</i> | NSY ATG11Δ::KAN TRS85Δ::HYGRO | This study |
|---------|--------------------------------------|-------------------------------|------------|

Table S2. Plasmids used in this study

| Plasmid | Alias | Genotype | Source |
|----------------|--------------|--|---------------|
| pNS196 | pACT2 | 2 μ , <i>LEU2</i> , Amp ^r | Clontech, CA |
| pNS1377 | | pACT2- <i>YPT1</i> | This study |
| pNS1378 | | pACT2- <i>YPT1-T40K</i> | This study |
| pNS1375 | | pACT2- <i>YPT1-S22N</i> | This study |
| pNS1374 | | pACT2- <i>YPT1-Q67L</i> | This study |
| pNS1376 | | pACT2- <i>YPT1-D124N</i> | This study |
| pNS206 | pGBDU-C2 | 2 μ , <i>URA3</i> , Amp ^r | [1] |
| pNS1373 | | pGBDU-C2- <i>ATG11</i> | This study |
| pNS1385 | | pGBDU-C2- <i>ATG11-CC2-3</i> | This study |
| pNS1386 | | pGBDUC1- <i>ATG11ΔCC1</i> | This study |
| pNS1387 | | pGBDU-C1- <i>ATG11ΔCC2</i> | This study |
| pNS1388 | | pGBDU-C1- <i>ATG11ΔCC3</i> | This study |
| pNS1389 | | pGBDU-C1- <i>ATG11ΔCC4</i> | This study |
| pNS1390 | | pGBDU-C2- <i>SEC4-Q79L</i> | This study |
| pNS1391 | | pGBDU-C2- <i>YPT31-Q72L</i> | This study |
| pNS1392 | | pGBDU-C2- <i>YPT6-Q69L</i> | This study |
| pNS1348 | pBS10 | Cerulean- <i>HYGRO</i> , Amp ^r | [6] |
| pNS1320 | pBS34 | mCherry- <i>KAN</i> , Amp ^r | [7] |
| pNS719 | pRS317 | <i>CEN</i> , <i>LYS2</i> , Amp ^r | [8] |
| pNS243 | pRS313 | <i>CEN</i> , <i>HIS3</i> , Amp ^r | [9] |
| pNS245 | pRS315 | <i>CEN</i> , <i>LEU2</i> , Amp ^r | [9] |
| pNS1359 | | p416-yEGFP- <i>ATG11</i> | This study |
| pNS1360 | | p416-yEGFP- <i>ATG8</i> | This study |

| | | |
|---------|--|------------|
| pNS1361 | p416-yEGFP- <i>ATG1</i> | This study |
| pNS1340 | p416-VF1 | [10] |
| pNS1341 | p415-VF2 | [10] |
| pNS1362 | p416-mCherry- <i>ATG8</i> | This study |
| pNS1364 | pRS315- <i>YPT1</i> | This study |
| pNS1365 | pRS315- <i>YPT1-T40K</i> | This study |
| pNS1366 | pRS315- <i>ATG11-YPT1</i> | This study |
| pNS1367 | pRS315- <i>ATG11-YPT1-T40K</i> | This study |
| pNS1368 | pRS317- <i>YPT1</i> | This study |
| pNS1369 | pRS317- <i>YPT1-T40K</i> | This study |
| pNS1370 | pRS317- <i>ATG11-YPT1</i> | This study |
| pNS1371 | pRS317- <i>ATG11-YPT1-T40K</i> | This study |
| pNS1372 | pRS317- <i>YPT1</i> promoter- <i>ATG11-YPT1</i> terminator | This study |
| pNS1380 | p413-Y/CFP C- <i>YPT1</i> | This study |
| pNS1381 | p413-Y/CFP C- <i>YPT1-T40K</i> | This study |
| pNS1382 | p413-Y/CFP C- <i>YPT1-Q67L</i> | This study |
| pNS1383 | p416-YFP N- <i>ATG11</i> | This study |
| pNS1384 | p415- <i>TRS85</i> -CFP N | This study |
| pNS1412 | p416-YFP N- <i>ATG11ACC2</i> | This study |

| | | | |
|---------|-------|--|-------------------------|
| pNS1413 | | p416-YFP N- <i>ATG11ΔCC3</i> | This study |
| pNS1409 | | p415- <i>ATG19</i> -Y/CFP C | This study |
| pNS1410 | | p416-YFP N- <i>ATG1</i> | This study |
| pNS1411 | | p413-Y/CFP C- <i>ATG1</i> | This study |
| pNS274 | YEp24 | 2 μ , <i>URA3</i> , Amp ^r | New England Biolabs, MA |
| pNS489 | | YEp24- <i>YPT1</i> | [11] |
| pNS229 | | YEp24- <i>YPT31</i> | [12] |

Supplementary Figure Legends

Figure S1. Yeast-two hybrid interaction with Ypt1 requires coiled-coil CC2 and CC3 of Atg11.

Ypt1 and Ypt1-GTP (Q67L) were cloned into the AD vector. Atg11 and mutants missing one of its four coiled-coil domains, CC1, CC2, CC3, or CC4, were cloned into the BD vector. Both the wild type and the GTP-restricted form of Ypt1 interact with Atg11, Atg11 Δ CC1 and Δ CC4, but not with Atg11 Δ CC2 and Δ CC3. Bottom: Immuno-blot analysis shows expression of the Atg11 proteins.

Figure S2. Ypt1, Trs85 and Atg11 localization and multicolor BiFC controls.

A. The intra-cellular localization of the Ypt1-1 mutant protein is similar to that of the wild type. Ypt1 localization was determined by immuno-fluorescence microscopy using anti-Ypt1 antibody in wild type (top) and *ypt1-1* mutant (bottom) cells. **B.** Atg1 shows positive PCA with Atg11 but not with Ypt1. BiFC is seen only for Atg1 and Atg11 (right), but not for Atg1 and Ypt1 (left). **C.** Atg11-CC2 and Atg11-CC3 are required for BiFC of Atg11 with Ypt1. BiFC with Ypt1 is seen only when YFP-N is tagged to Atg11 wild type, and not to Atg11 Δ CC2 or Atg11 Δ CC3 (left panels). In contrast, BiFC with Atg19 is seen for wild type Atg11, Atg11 Δ CC2 and Atg11 Δ CC3 tagged with YFP-N (right panels). **D.** Localization of Trs85 to multiple puncta. Endogenous Trs85 tagged at its C-terminus with GFP localizes to multiple puncta (left). Trs85-GFP is functional (right): Yeast cells expressing Trs85-GFP from the chromosome are resistant to nitrogen starvation. Yeast cells carrying wild type *TRS85* (as a positive control), *TRS85*-GFP, or *trs85* Δ allele (as a negative control), were shifted to medium without nitrogen and

viability was tested at the indicated times. Viability is shown as percent of viability in day zero. Whereas *trs85Δ* cells are sensitive to nitrogen starvation, cells expressing Trs85-GFP are as resistant as wild type cells.

Figure S3. Quantification of GFP-tagged Atg11, Atg8 and Atg1 proteins in wild type and *ypt1-1* mutant cells. **A.** Quantification of micrographs used for Figure 3A. **B.** The level of proteins used for microscopy in Figure 3A was determined by immuno-blot analysis using anti-GFP antibody (G6PDH is shown as a loading control). **C.** Quantification of micrographs used for Figure 3C.

Figure S4: The role of Ypt1, Trs85 and Atg11 in autophagy. **A.** Over expression of Ypt1, but not Ypt31, can suppress the Ape1 processing defect of *trs85Δ* mutant cells. The experiment was done as described in Figure 4A, except that *trs85Δ* cells were transformed with a 2μ empty plasmid (-), a plasmid over-expressing Ypt1 (1) or Ypt31 (31). **B.** The growth defect during nitrogen starvation of the *atg11Δtrs85Δ* double deletion mutant cells is not more severe than that of the single deletion mutants. The viability of wild type, *atg11Δ*, *trs85Δ*, *atg11Δtrs85Δ*, and *ypt1-1* mutant cells, was determined before and after the shift to medium without nitrogen. Shown is the percent of live cells two and four days after the shift compared to the number of cells before the shift. Both *atg11Δ* and *trs85Δ* single deletion cells exhibit an intermediate nitrogen-starvation growth phenotype between that of the wild type and *ypt1-1* mutant cells. The *trs85Δ atg11Δ* double deletion mutant cells exhibit a growth defect similar to that of *trs85Δ*. **C.** Trs85-GFP co-localizes with Atg9-mCherry. Endogenous Trs85 and Atg9 were tagged on the chromosome with GFP and mCherry, respectively.

Shown from left to right: DIC, GFP, mCherry, and merge. All the Trs85 green puncta overlap with the red Atg9 puncta (arrows). There are more Atg9 red puncta than the Trs85 green puncta (arrow heads). **D.** The localization pattern of Atg9 is altered in *ypt1-1* and *trs85Δ* mutant cells. Endogenous Atg9 was tagged on the chromosome with mCherry and cells were visualized in the mCherry channel. The number of Atg9 dots per cell (column graph at the bottom, at least 200 cells were visualized for each strain) is lower in *trs85Δ* and *ypt1-1* mutant cells as compared to wild type cells.

Figure S5: The Trs85 and Ypt1 PCA puncta do not overlap with secretory compartment markers. The experiment was done as described in Figure 2C, except that the following compartmental markers were tagged on the chromosome with RFP: Sec13-ER-ES (ER exit sites), COP1-cis Golgi, Anp1-Golgi, Chc1-trans Golgi, Snf7-endosomes [19]. Cells were visualized in the CFP and RFP channels. The blue (CFP) puncta do not overlap with red (RFP) fluorescence (merge) indicating that the Trs85-Ypt1 interaction does not occur in the ER, Golgi or endosomes. DIC is shown in the left column.

References

1. James, P., J. Halladay, and E.A. Craig, *Genomic libraries and a host strain designed for highly efficient two-hybrid selection in yeast*. Genetics, 1996. 144(4): p. 1425-36.
2. Jedd, G., J. Mulholland, and N. Segev, *Two new Ypt GTPases are required for exit from the yeast trans-Golgi compartment*. J Cell Biol, 1997. 137(3): p. 563-80.
3. Baker, D., L. Wuestehube, R. Schekman, D. Botstein, and N. Segev, *GTP-binding Ypt1 protein and Ca²⁺ function independently in a cell-free protein transport reaction*. Proc Natl Acad Sci U S A, 1990. 87(1): p. 355-9.
4. Brachmann, C.B., A. Davies, G.J. Cost, E. Caputo, J. Li, P. Hieter, and J.D. Boeke, *Designer deletion strains derived from Saccharomyces cerevisiae S288C: a useful set of strains and plasmids for PCR-mediated gene disruption and other applications*. Yeast, 1998. 14(2): p. 115-32.
5. Noda, T., A. Matsuura, Y. Wada, and Y. Ohsumi, *Novel system for monitoring autophagy in the yeast Saccharomyces cerevisiae*. Biochem Biophys Res Commun, 1995. 210(1): p. 126-32.
6. Rizzo, M.A., G.H. Springer, B. Granada, and D.W. Piston, *An improved cyan fluorescent protein variant useful for FRET*. Nat Biotechnol, 2004. 22(4): p. 445-9.
7. Shaner, N.C., R.E. Campbell, P.A. Steinbach, B.N. Giepmans, A.E. Palmer, and R.Y. Tsien, *Improved monomeric red, orange and yellow fluorescent proteins derived from Discosoma sp. red fluorescent protein*. Nat Biotechnol, 2004. 22(12): p. 1567-72.
8. Eriksson, P., L.R. Thomas, A. Thorburn, and D.J. Stillman, *pRS yeast vectors with a LYS2 marker*. Biotechniques, 2004. 36(2): p. 212-3.
9. Sikorski, R.S. and P. Hieter, *A system of shuttle vectors and yeast host strains designed for efficient manipulation of DNA in Saccharomyces cerevisiae*. Genetics, 1989. 122(1): p. 19-27.
10. Paquin, N., M. Menade, G. Poirier, D. Donato, E. Drouet, and P. Chartrand, *Local activation of yeast ASH1 mRNA translation through phosphorylation of Khd1p by the casein kinase Yck1p*. Mol Cell, 2007. 26(6): p. 795-809.
11. Morozova, N., Y. Liang, A.A. Tokarev, S.H. Chen, R. Cox, J. Andrejic, Z. Lipatova, V.A. Sciorra, S.D. Emr, and N. Segev, *TRAPP II subunits are required for the specificity switch of a Ypt-Rab GEF*. Nat Cell Biol, 2006. 8(11): p. 1263-9.
12. Jones, S., G. Jedd, R.A. Kahn, A. Franzusoff, F. Bartolini, and N. Segev, *Genetic interactions in yeast between Ypt GTPases and Arf guanine nucleotide exchangers*. Genetics, 1999. 152(4): p. 1543-56.
13. Longtine, M.S., A. McKenzie, 3rd, D.J. Demarini, N.G. Shah, A. Wach, A. Brachat, P. Philippsen, and J.R. Pringle, *Additional modules for versatile and economical PCR-based gene deletion and modification in Saccharomyces cerevisiae*. Yeast, 1998. 14(10): p. 953-61.

14. Wach, A., A. Brachat, R. Pohlmann, and P. Philippsen, *New heterologous modules for classical or PCR-based gene disruptions in Saccharomyces cerevisiae*. *Yeast*, 1994. 10(13): p. 1793-808.
15. Wach, A., A. Brachat, C. Alberti-Segui, C. Rebischung, and P. Philippsen, *Heterologous HIS3 marker and GFP reporter modules for PCR-targeting in Saccharomyces cerevisiae*. *Yeast*, 1997. 13(11): p. 1065-75.
16. Sheff, M.A. and K.S. Thorn, *Optimized cassettes for fluorescent protein tagging in Saccharomyces cerevisiae*. *Yeast*, 2004. 21(8): p. 661-70.
17. Taxis, C. and M. Knop, *System of centromeric, episomal, and integrative vectors based on drug resistance markers for Saccharomyces cerevisiae*. *Biotechniques*, 2006. 40(1): p. 73-8.
18. Hu, C.D. and T.K. Kerppola, *Simultaneous visualization of multiple protein interactions in living cells using multicolor fluorescence complementation analysis*. *Nat Biotechnol*, 2003. 21(5): p. 539-45.
19. Huh, W.K., J.V. Falvo, L.C. Gerke, A.S. Carroll, R.W. Howson, J.S. Weissman, and E.K. O'Shea, *Global analysis of protein localization in budding yeast*. *Nature*, 2003. 425(6959): p. 686-91.

Figure S1

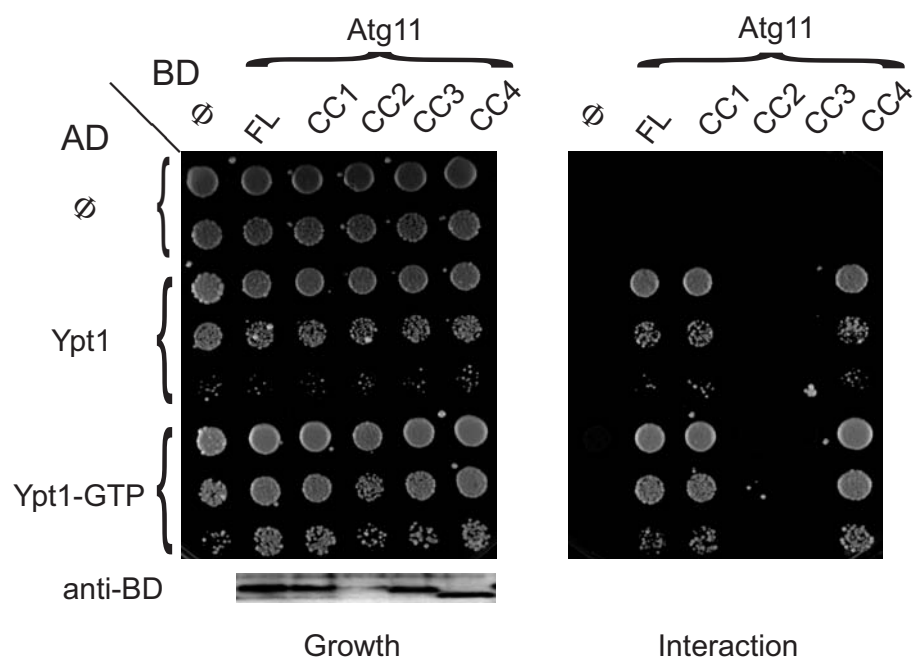
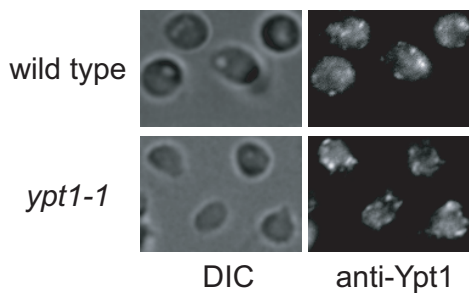
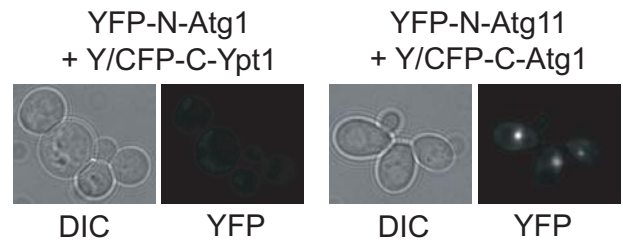


Figure S2

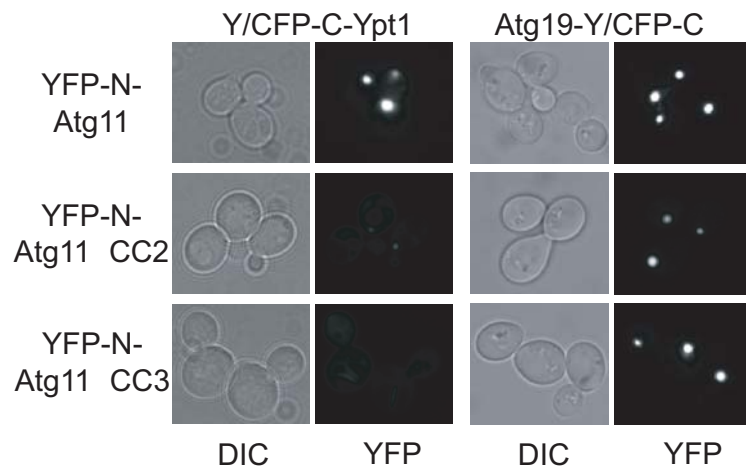
A.



B.



C.



D.

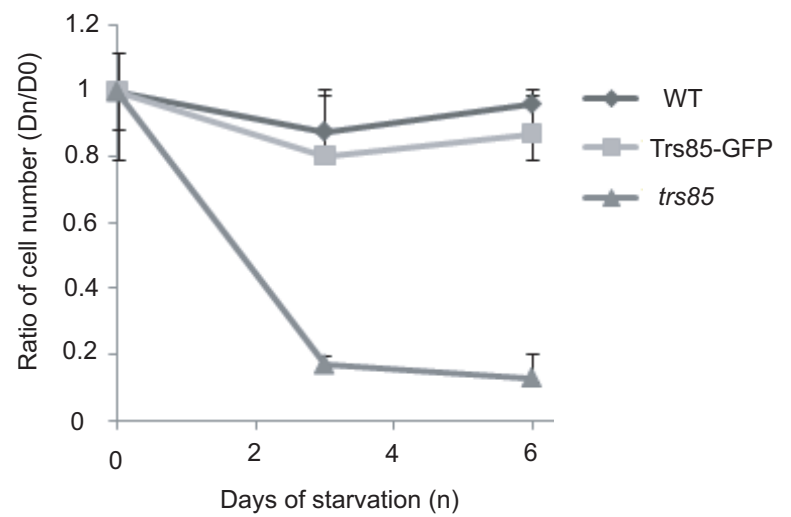
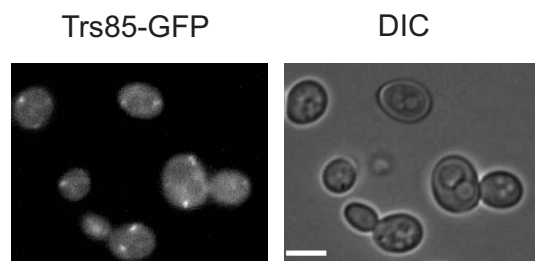
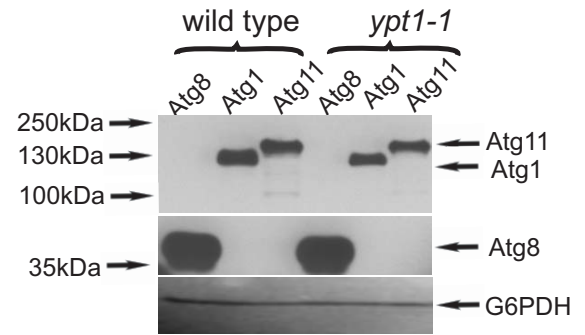


Figure S3

A.

| | measured | strain | # cells | % |
|-----------|-------------|---------------|---------|----|
| GFP-Atg11 | > 1dot/cell | wild type | 100 | 15 |
| | | <i>ypt1-1</i> | 100 | 71 |
| GFP-Atg8 | > 1dot/cell | wild type | 100 | 12 |
| | | <i>ypt1-1</i> | 100 | 94 |
| GFP-Atg1 | no dot | wild type | 100 | 18 |
| | | <i>ypt1-1</i> | 100 | 84 |

B.



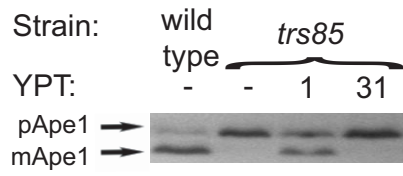
C.

| Ypt/Atg11 plasmid | ∅ | Ypt1 | Atg11-Ypt1 | Ypt1-1 | Atg11-Ypt1-1 | Atg11 |
|------------------------|----|------|------------|--------|--------------|-------|
| % GFP-Atg1 no dot | 84 | 20 | 40 | 82 | 44 | 86 |
| % GFP-Atg8 > 1dot/cell | 94 | 12 | 44 | 94 | 46 | 86 |

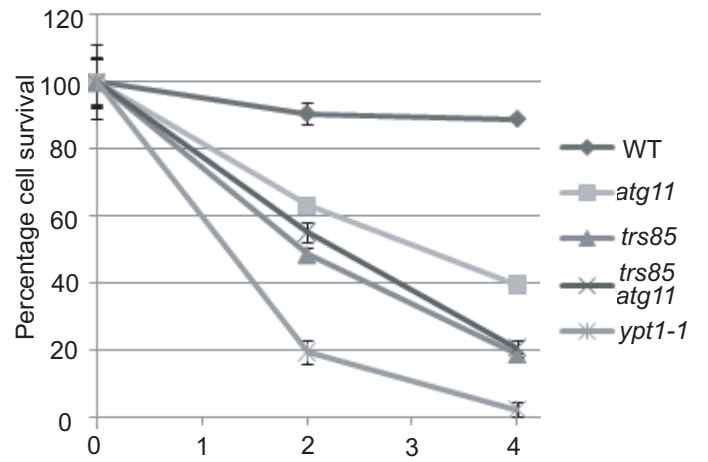
50 cells scored for each strain

Figure S4

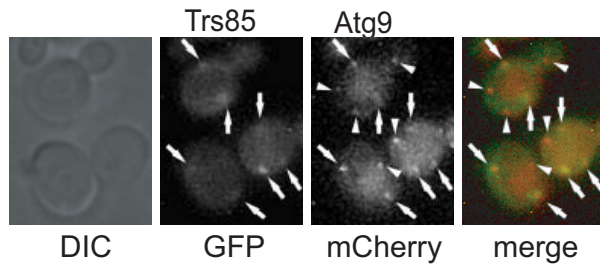
A.



B.



C.



D.

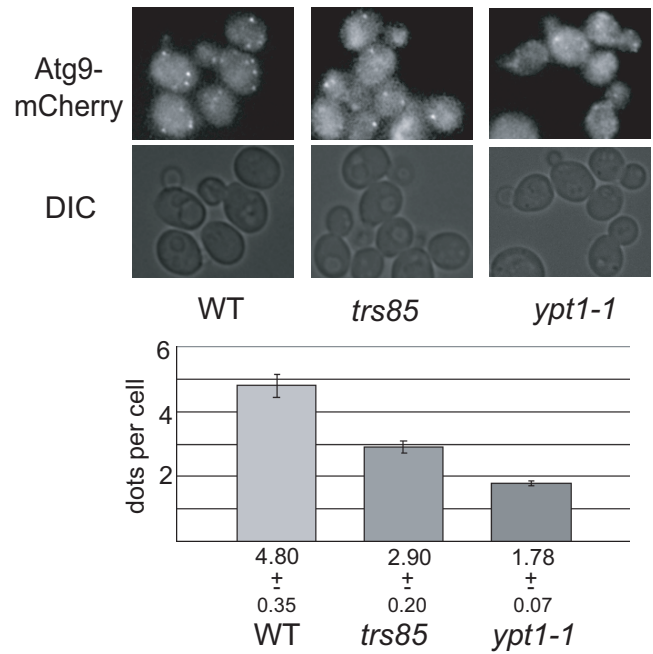


Figure S5

